NANO LETTERS

2007
Vol. 7, No. 6
1779−1784

Multiple Exciton Generation in Films of Electronically Coupled PbSe Quantum Dots

Joseph M. Luther,*,†,‡ Matthew C. Beard,*,† Qing Song,† Matt Law,† Randy J. Ellingson,† and Arthur J. Nozik*,†,§

Chemical and Biosciences Center, National Renewable Energy Laboratory, Golden, Colorado 80401, Department of Applied Physics, Colorado School of Mines, Golden, Colorado 80401, and Department of Chemistry and Biochemistry, University of Colorado, Boulder, Colorado 80309

Received April 12, 2007; Revised Manuscript Received May 7, 2007

ABSTRACT

We study multiple exciton generation (MEG) in electronically coupled films of PbSe quantum dots (QDs) employing ultrafast time-resolved transient absorption spectroscopy. We demonstrate that the MEG efficiency in PbSe does not decrease when the QDs are treated with hydrazine, which has been shown to greatly enhance carrier transport in PbSe QD films by decreasing the interdot distance. The quantum yield is measured and compared to previously reported values for electronically isolated QDs suspended in organic solvents at ∼4 and 4.5 times the effective band gap. A slightly modified analysis is applied to extract the MEG efficiency and the absorption cross section of each sample at the pump wavelength. We compare the absorption cross sections of our samples to that of bulk PbSe. We find that both the biexciton lifetime and the absorption cross section increase in films relative to isolated QDs in solution.

Conventional single-junction solar cells waste the energy of absorbed photons in excess of the band gap as heat. One way to reduce this undesirable heat generation is to produce multiple electron−hole pairs, or excitons, from those photons possessing an energy greater than at least twice the effective band gap.[1] The process of creating multiple excitons from single photons, known as multiple exciton generation (MEG),[2] has been demonstrated in colloidal suspensions of PbSe, PbS, PbTe, CdSe, and InAs nanocrystals, or quantum dots (QDs).[3−7] A maximum theoretical efficiency of 42% is predicted for single-junction devices employing MEG-active absorbers, compared with 33% for normal absorbers.[8] Extracting the photogenerated charges from MEG-active quantum dots is a critical challenge to the fabrication of efficient MEG solar cells.

To date, all reported measurements of MEG have been based on QDs suspended in solution, electronically isolated from one another. However, for high efficiency in certain MEG QD solar cell designs, the QDs must be electronically coupled such that charge separation occurs on a time scale longer than MEG ($\sim 10^{-13}-10^{-12}$ s) but shorter than the biexciton lifetime ($\sim 10^{-10}$ s). The charges must then drift and/or diffuse to the electrodes before recombining. Colloidal QD solar cells[1] based on QD-sensitized nanocrystalline TiO_2 and QD−polymer blends have been demonstrated.[9−14] In these types of devices, removal of the electrically insulating ligand shell surrounding each QD is vital for optimizing charge injection and can be accomplished with solution-based ligand exchange procedures.[15,16] In another, perhaps more promising device geometry,[1] an ordered three-dimensional QD film forms the intrinsic region of a p−i−n structure in which extended states, formed from the coupled QDs, allow for the delocalized photogenerated carriers to traverse the film and be collected in the doped regions, which may be heavily doped bulk semiconductors. Exchanging the bulky capping ligands used in the QD synthesis with shorter molecules after film formation can drastically increase the carrier mobility of QD films[17−21] by reducing the interdot spacing[22] while retaining relatively highly passivated surfaces, thus achieving the most intimate contact shy of sintering the particles together. Distinct excitonic features can still be preserved with these electronic coupling techniques and, although this type of coupling may be necessary for the efficient extraction of carriers from a film, it was not known how well MEG is preserved in coupled QD films. It is important to understand how the enhanced delocalization of the excitons affects the MEG quantum yield (QY). In this work, we investigate the influence of electronic coupling on

* Corresponding authors. E-mail: joseph_luther@nrel.gov; matt_beard@nrel.gov; arthur_nozik@nrel.gov.
† National Renewable Energy Laboratory.
‡ Colorado School of Mines.
§ University of Colorado.

10.1021/nl0708617 CCC: $37.00
Published on Web 05/27/2007

the exciton yield upon absorption of high-energy photons in PbSe QD films.

Trioctylphosphine (TOP, technical grade, >90%) was purchased from Fluka. Lead oxide, selenium powder (100 mesh, 99.99%), oleic acid (OA, technical grade, 90%), 1-octadecene (ODE, 90%), anhydrous hexane, anhydrous methanol, acetone, and tetrachloroethylene (TCE, HPLC grade, 99.9+%) were purchased from Aldrich. All chemicals were used without further purification. A 1 M TOP−Se stock solution was prepared by dissolving 0.1 mol of selenium in 100 mL of TOP at room temperature and stored in an inert atmosphere.

PbSe QDs were synthesized by a slightly modified literature procedure.[5,23] In a typical synthesis, 1 mmol of PbO was dissolved in a mixture of 2.25 mmol of OA and 4 g of ODE at 150 °C to make a clear solution. Once the solution temperature reached 180 °C, 2 mL of 1 M TOP−Se was swiftly injected and allowed to react until the desired size QD was achieved. The solution was then cooled to room temperature and 3 mL of anhydrous hexane was added. The dots were extracted by addition of anhydrous methanol and then precipitated with acetone. They were washed several times by sequential dispersion in anhydrous hexane and precipitation with acetone. Finally, the QDs were dispersed in chloroform with a concentration of ~100 mg/mL for film preparation.

Unless otherwise stated, all fabrication and treatments of PbSe QD films occurred in either helium or argon gloveboxes to prevent oxidation. Glass substrates (0.5 in.^{2}) were sequentially cleaned with 2-propanol, acetone, and chloroform in an ultrasonic bath. After the PbSe QDs were spin-coated at 1000 rpm, they were dried overnight and then kept under a dynamic vacuum for 12 h to remove residual solvent. The resulting films were chemically treated by soaking in 1 M hydrazine in acetonitrile for 20−24 h.[17,18] Treating the films with other amines including aniline, pyridine, methylamine, butylamine, and ethylenediamine produced undesirable effects such as insignificant coupling enhancement, substantial grain growth during ligand exchange, or very fast single exciton lifetimes. For laser measurements the films were sealed in a helium-filled sample cell between sapphire windows. Optical absorption data were collected with a Shimadzu UV-3600 spectrophotometer equipped with an integrating sphere. Photoluminescence data were acquired using a PTI QuantaMaster NIR luminescence spectrometer with a liquid N_2 cooled InGaAs detector and a Spectra Physics Tsunami Ti:sapphire laser as the excitation source. Scanning electron microscopy (SEM) was performed on a JEOL JSM-7000F field emission scanning electron microscope.

We studied ~150 nm thick films composed of QDs with first exciton transitions at 0.80, 0.84, and 0.90 eV, corresponding to QD radii of 2.45, 2.27, and 2.03 nm, respectively. The 150 nm thick films correspond to an optical density of roughly 0.2 at the first exciton. Figure 1 shows the room temperature absorbance and emission of the 0.90 eV QD films. The true absorbance is obtained from the measured transmission and reflection spectra, which were collected

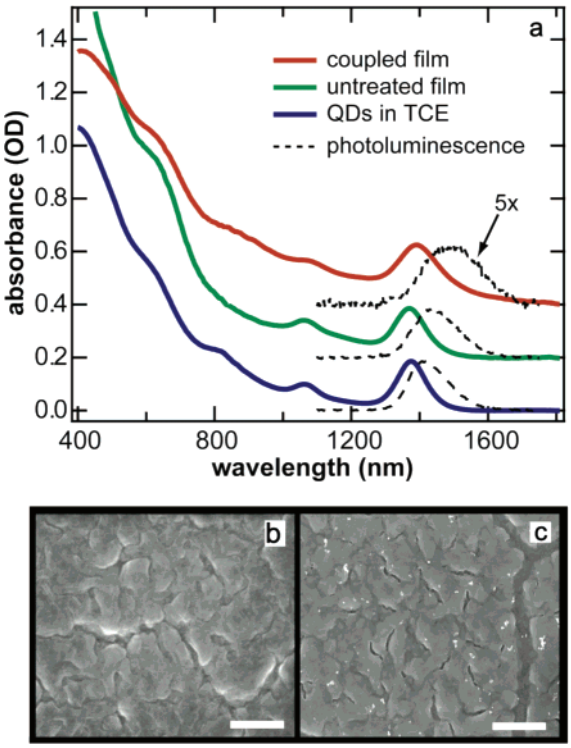

Figure 1. (a) Absorbance (solid) and photoluminescence (dotted) for PbSe QDs (E_g = 0.90 eV) in TCE (blue), cast as a film (green), and cast as a film and treated with hydrazine (red). The photoluminescence of the treated film is magnified 5-fold and all curves are offset for clarity. SEM images which show the morphology of an untreated film (b) and a coupled film (c). The scale bar is 1 μm in both images.

using an integrating sphere to eliminate erroneous peak positions that can occur due to scattering.[24] The excitonic absorbance features of the films prior to treatment are similar to that of isolated QDs in solution. The hydrazine treatment causes the lowest energy transition to red shift by ~16 meV (20 nm) and broaden (see the first exciton peak in Figure 1a). A red shift can arise from exciton delocalization, dipole−dipole interactions, which would lower the transition energy, or differences in dielectric screening in the films compared to solution.[24−26] These descriptions are all governed by dielectric properties that change with the alteration of the capping group. The broadening has been previously explained in QD solids by electronic coupling, causing a splitting of quantized energy levels as the interdot distance decreases.[27] We believe a combination of classical and quantum mechanical effects is responsible for the red shift and broadening in our films. Classical dipole−dipole interactions and the self-polarization energy, which account for solvochromatic shifts in colloidal CdSe NCs,[28] can only account for a red shift of approximately 2−8 meV in a close packed PbSe film where the QDs are in intimate contact, much smaller than our measured values. SEM images were used to compare film morphology before and after treatment (Figure 1b,c). QDs cluster in tight-packed domains of 400 nm and upon treatment, 60−200 nm long pits form between the domains at the grain boundary, where the capping ligand is most easily reached by hydrazine.

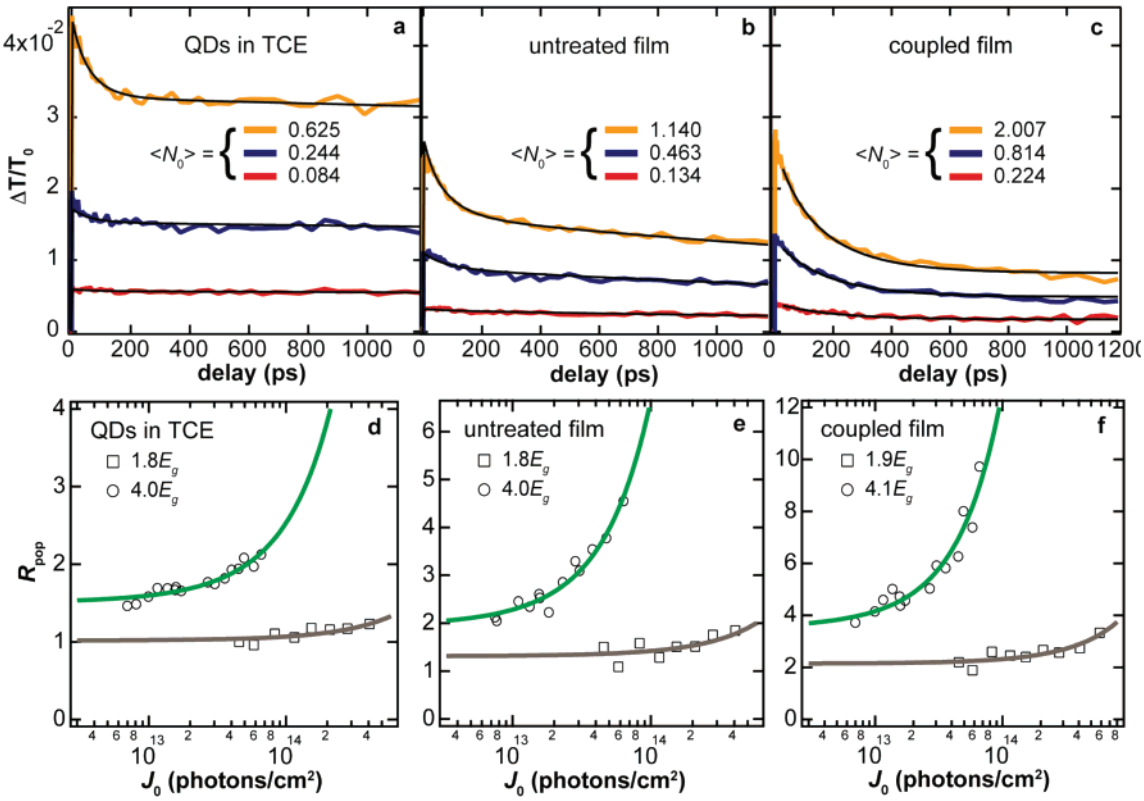

Figure 2. Transient absorption dynamics and analysis for PbSe QDs in a solution, untreated film, and a coupled film treated with 1 M hydrazine for 24 h. (a−c) Transient absorption signals at three different pump powers for each sample (13.7 (red), 62.4 (blue), and 136.8 mW/cm^2 (orange)). The global fit lines are shown in black. (d−f) Ratio of exciton population at 3 to 750 ps after excitation with pump energy of $<2E_g$ (squares) and $\sim 4E_g$ (circles) for varying pump fluence. The fits to these data are described in the text.

The transient absorption (TA) apparatus used to quantify MEG in the films consists of an amplified Ti:sapphire laser (Integra-E, Quantronix Inc.) seeded by a wide bandwidth Ti:sapphire oscillator (MK Labs, Chinook). The amplified laser produces ∼60 fs full width at half-maximum pulses centered at 810 nm with a 1 kHz repetition rate, which pumps two independently tunable optical parametric amplifiers (TOPAS, Light Conversion) producing visible and NIR pulses for the respective pump and probe arms of the TA apparatus. The probe wavelength is chosen to be resonant with the first exciton absorption transition of the QD sample. The typical pump and probe spot diameters are 600 and 100 μm, respectively. Passing the pump beam through a synchronous chopper (New Focus model 3501) phase-locked to the laser pulse train (500 Hz, blocking every other pump pulse) enables amplitude measurement of the transmitted probe pulse with and without the pump pulse present. Comparison of the probe intensity with and without the pump permits calculation of the differential transmission, $\Delta T/T_0$. Measurements made by varying the relative optical delay between the pump and probe pulses produce the time-dependent data shown in Figure 2.

The decay dynamics of the single exciton were studied by photoexciting below the minimum MEG threshold of $2E_g$ with 810 nm light. Figure 2a−c displays the TA of QDs with a 0.84 eV band gap dispersed in solution and the films of QDs for three different pump fluences, 5.5×10^{13}, 2.5×10^{14}, and 5.5×10^{14} photons/cm^2 per pulse. $\Delta T/T_0$ is measured at a 3 and 750 ps delay with respect to the pump beam, and the ratio of these two values, R_{pop}, is plotted versus the average pump fluence in parts d−f of Figure 2. The samples were photoexcited below the MEG threshold ($<2E_g$), as well as $\sim 4E_g$, such that the QY of exciton generation could be determined.

The single exciton lifetime (τ_1) is modeled as a single exponential. Using sub-MEG-threshold excitation, the weakest pump pulse TA curve shows little evidence of Auger recombination and yields a value of $\tau_1 > 30$ ns for the QDs suspended in TCE. This excitation yields an average per dot exciton population, $\langle N_0 \rangle$, of 0.084, and assuming a Poisson distribution corresponds to <5% of the excited QDs absorbing multiple photons. The single exciton lifetime decreases to 4 ns for an untreated film and 1.7 ns for a coupled film. This lifetime is usually controlled by the presence of recombination sites at the surface of the QD. A large single exciton lifetime reduction is seen in PbSe QD films compared with the QDs in TCE, which may be caused by breaking bonds between capping ligands and the QD surface during film preparation. In solution, the surface is surrounded by molecules which may dynamically passivate dangling bonds or other surface trapping centers. As a solid film, surface passivation of this nature cannot prevail, leading to increased recombination. In general, amines should provide better surface state passivation than OA; this feature was used to partially explain the increase in photoconductivity for similarly treated CdSe[29] and PbSe QD[18] films. However, unlike the inference in refs 18 and 29 that the single exciton lifetime would be expected to increase, we find that the single

Table 1. The Single (τ_1) and Biexciton (τ_2) Lifetimes, Absorption Cross Section (σ) at 800 nm, and Exciton QY for Samples of 0.84 and 0.90 eV PbSe QDs

	QDs in TCE		untreated film		coupled film	
	0.84 eV	0.90 eV	0.84 eV	0.90 eV	0.84 eV	0.90 eV
τ_1 (ns)	>30	>100	4.1	4.5	1.7	2.7
τ_2 (ps)	67	42	88	125	116	130
σ_{800nm} (cm^2)	9.7×10^{-16}	1.33×10^{-15}	1.6×10^{-15}	2.81×10^{-15}	1.6×10^{-15}	3.12×10^{-15}
QY[a] (%)	148	209	148	211	164	225

[a] QY for the 0.84 eV sample was measured with a pump energy $\sim 4E_g$. The 0.90 eV sample was pumped at $\sim 4.5E_g$ where MEG is more efficient.

exciton lifetime *decreases* upon treatment in hydrazine, indicating a reduced effective surface passivation. This might be partially explained by an incomplete coverage of surface passivating molecules in our films relative to QDs in solution. Other PbSe film properties, such as morphology and ordering, are highly dependent on postsynthesis cleaning procedures that determine the coverage of the capping molecules on the QDs.[19] We envision that specific sample-dependent cleaning procedures affect the single exciton lifetime, the degree of coupling between QDs, and packing of the QDs in the film. One initial sample oxidized during our studies, and a drastic change was noted in the single exciton dynamics, demonstrating how the surface can significantly alter the properties of the QDs. Absorbance measurements confirmed that oxidation of this sample had occurred.[30]

A fit was applied to each of the data sets in Figure 2a−c in which the single exciton decay dynamics are held constant and the biexciton lifetime is varied globally, and the average number of photons absorbed per QD, $\langle N_o \rangle$, is extracted for each excitation intensity. Table 1 displays the single exciton and biexciton lifetimes for QDs in TCE, cast as a film, and for the coupled array for two different QD sizes. The biexciton lifetime for the 0.84 eV sample increases from 67 to 116 ps between the solution and the films, while the 0.90 eV sample displays an increase from 42 to 130 ps. The slight variation in the biexciton lifetime is apparently due to the sample treatment and passivating conditions; however, all films show biexciton lifetimes significantly longer than those measured for isolated QDs in solution.

The increased biexciton lifetime in coupled QDs can be explained by delocalization of the exciton wave function. The biexciton lifetime is proportional to the interaction volume. Figure 3a displays measured biexciton lifetimes for QDs of different size, and a linear trend as a function of volume is observed, consistent with previous reports.[3] Upon coupling of QDs, the biexciton lifetime deviates from this linear dependence as noted by the arrows. The coupled film deviates more than the untreated one, which suggests that the exciton confinement radius increases by as much as 45% in the coupled film. We note that this increase in biexciton lifetime is not equivalent to assuming the effective QD volume increases accordingly. An equivalent biexciton lifetime for isolated QDs would correspond to an effective band gap less than 0.5 eV; in contrast, the effective band gap of the coupled film is clearly much larger (0.8 − 0.9 eV) (see Figure 1). The decrease in exciton confinement results in the formation of extended states such that multiple

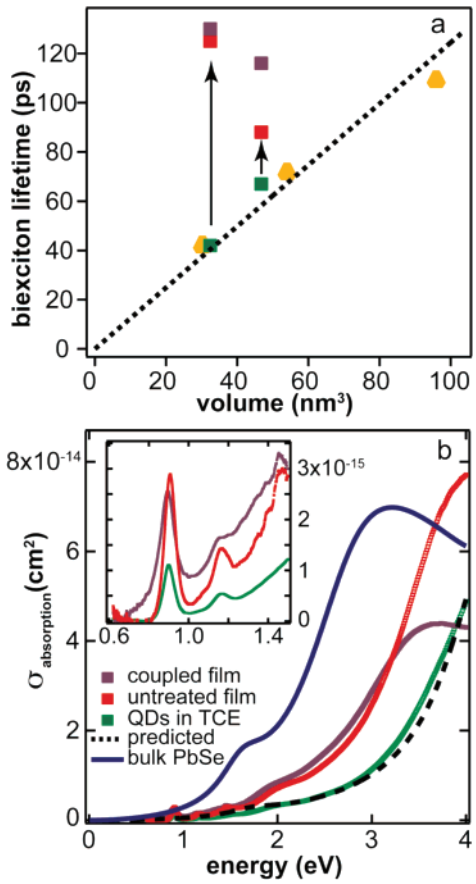

Figure 3. (a) The biexciton lifetime in TCE as a function of volume for several PbSe QD sizes (orange) including QDs used in this study (green). Once the QDs are cast into films (red) and coupled (violet), the biexciton lifetime increases (shown by the arrow) from the linear dependence observed for QDs in solution (dotted line). (b) The absorption cross section of bulk PbSe compared with samples measured in this work. The solution prediction is calculated using the displayed bulk values but adjusted for differences in the dielectric environment. The inset shows the excitonic features of the samples.

excitons require more time to interact and undergo Auger recombination, a feature beneficial to efforts to collect charge following MEG.

The generation of multiple excitons occurs on a time scale at least 2 to 3 orders of magnitude faster than the Auger recombination rate.[4,31] This suggests that excitons must be separated into charge carriers 1−100 ps after photon absorption for efficient collection of charges from all generated excitons.[31,32] Long-range mobilities for similar PbSe films have been reported ~ 1 cm^2 $(V \cdot s)^{-1}$.[18] In a typical p−i−n

device structure with highly doped quasi-neutral regions and a built-in field of 1 V across a 1 μm intrinsic QD layer, the time required for an electron to drift 5 nm (onto another QD) is ~50 ps. The increased biexciton lifetime in coupled films provides ample time for this process to occur.

The observation of MEG using TA relies on the fact that Auger recombination is much faster than single exciton recombination. Here, we use the same technique as previously reported[3−6] to deduce exciton generation efficiency with only a slight alteration of the data analysis. The analysis proceeds as follows. The ratio of normalized change in transmission soon after the excitation pulse (3 ps) to that after all Auger recombination is complete (750 ps) is plotted versus photon fluence and the following equation is fit to the data

$$R_{\mathrm{pop}} = \frac{\left(\frac{\Delta T}{T_0}\right)_{t=3\mathrm{ps}}}{\left(\frac{\Delta T}{T_0}\right)_{t=750\mathrm{ps}}} = \frac{J_0\,\sigma\,\mathrm{QY}\,\delta}{1-\exp(-J_0\,\sigma)} \qquad (1)$$

where R_{pop} is defined as the ratio of exciton populations at 3 and 750 ps after excitation, J_0 is the photon fluence, σ is the absorbance cross section at the pump wavelength, QY is the number of excitons created per excited QD, and δ is the decrease in single exciton population over the time frame of the experiment (in this case, $e^{750-3(\mathrm{ps})/\tau_1}$). This analysis technique provides a reliable way to accurately determine the QY of exciton generation and also enables the direct measurement of the absorption cross section (σ) of the QDs in the films at the pump wavelength, which is a difficult but important parameter to measure.

In Figure 3b, we compare the bulk absorption cross section of an equivalent volume of PbSe[33] and the absorption cross section calculated for small crystals suspended in solution with increased dielectric screening[26] to that measured for the films and QDs in TCE. We find that the cross section of the films becomes more bulklike: this feature is most readily observed at high photon energies where the cross section in the films begins to significantly deviate from that found in solution. These observations are consistent with a reduced dielectric screening in the films relative to the solution. Knowledge of the absorption cross section is important for the MEG work reported here as well as future photovoltaic devices made from QD films.

Using this procedure, we have measured MEG efficiency in an untreated and an electronically coupled film compared with that of a solution of QDs in TCE from the same synthesis. In the sub-MEG-threshold case, a fit of eq 1 (gray line in Figure 2d−f) is applied where only σ and δ vary, and the QY is assumed to be 100%. Above the MEG threshold (green line in Figure 2d−f), δ is fixed at its sub-MEG-threshold value while the QY is allowed to vary. The best-fit value for the QY is found to be 148% at ~$4E_g$ for the QDs in TCE as well as in the untreated film and corresponds to the overall average efficiency of exciton generation in an excited QD. The coupled film has an exciton generation efficiency of 164% at ~$4E_g$. This slight increase

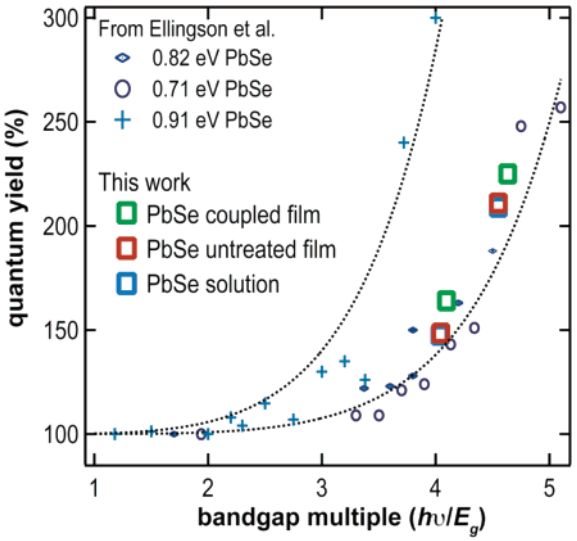

Figure 4. Quantum yield of exciton generation for PbSe QD films and QD solutions (from ref 4). The dotted lines are guides to the eye. Note that the QYs for QDs in solution and untreated films are identical.

in the coupled film arises, to some extent, from the slightly lower E_g of the coupled film while using the same pump wavelength for all measurements. The QY for the films used in this work is plotted in Figure 4 with previously reported[4] values for PbSe QDs in solution versus energy gap multiple. The QY results for coupled QD films are similar to what has been previously reported for isolated dots suspended in solvents. These results were all repeated using a smaller size of QDs with larger E_g (0.90 eV) from another synthesis. The QY agrees well with the first sample, and the same trend is observed regarding single exciton and the biexciton lifetimes, aside from the biexciton lifetime scaling with volume. These parameters for both QD sizes are displayed as a comparison in Table 1.

Using a post-film-fabrication soak treatment in 1 M hydrazine to electronically couple QDs in films, we have studied MEG efficiency of coupled PbSe QDs. We find no reduction of MEG in an electronically coupled QD film from that for isolated QDs in solution. Since MEG has only been shown to be efficient in QDs, we believe this is a particularly interesting result because one might hypothesize that treatments rendering the QDs to be more bulklike should greatly reduce the QY; however, an important issue yet to be answered is to what extent will MEG decrease upon further coupling, such as with annealing treatments that will eventually prevent quantum confinement. The ability to effectively couple QDs without reduction of MEG is very encouraging for the development of novel high-efficiency solar cells employing close-packed arrays of QDs.

Acknowledgment. The authors thank James Murphy, Justin Johnson, Kelly Knutsen, and Kathrine Gerth for helpful comments and experimental assistance in the preparation of this work. Funding is provided by the U.S. Department of Energy, Office of Basic Energy Sciences, Division of Chemical Sciences, Biosciences, and Geosciences.

References

(1) Nozik, A. J. *Physica E* **2002**, *14* (1−2), 115−120.
(2) Shabaev, A.; Efros, A. L.; Nozik, A. J. *Nano Lett.* **2006**, *6* (12), 2856−2863.
(3) Schaller, R. D.; Klimov, V. I. *Phys. Rev. Lett.* **2004**, *92* (18).
(4) Ellingson, R. J.; Beard, M. C.; Johnson, J. C.; Yu, P. R.; Micic, O. I.; Nozik, A. J.; Shabaev, A.; Efros, A. L. *Nano Lett.* **2005**, *5* (5), 865−871.
(5) Murphy, J. E.; Beard, M. C.; Norman, A. G.; Ahrenkiel, S. P.; Johnson, J. C.; Yu, P. R.; Micic, O. I.; Ellingson, R. J.; Nozik, A. J. *J. Am. Chem. Soc.* **2006**, *128* (10), 3241−3247.
(6) Schaller, R. D.; Sykora, M.; Jeong, S.; Klimov, V. I. *J. Phys. Chem. B* **2006**, *110* (50), 25332−25338.
(7) Pijpers, J. J. H.; Hendry, E.; Milder, M. T. W.; Fanciulli, R.; Savolainen, J.; Herek, J. L.; Vanmaekelbergh, D.; Ruhman, S.; Mocatta, D.; Oron, D.; Aharoni, A.; Banin, U.; Bonn, M. *J. Phys. Chem. C* **2007**, *111* (11), 4146−4152.
(8) Hanna, M. C.; Nozik, A. J. *J. Appl. Phys.* **2006**, *100* (7).
(9) Yu, P. R.; Zhu, K.; Norman, A. G.; Ferrere, S.; Frank, A. J.; Nozik, A. J. *J. Phys. Chem. B* **2006**, *110* (50), 25451−25454.
(10) Cui, D. H.; Xu, J.; Zhu, T.; Paradee, G.; Ashok, S.; Gerhold, M. *Appl. Phys. Lett.* **2006**, *88* (18).
(11) Robel, I.; Subramanian, V.; Kuno, M.; Kamat, P. V. *J. Am. Chem. Soc.* **2006**, *128* (7), 2385−2393.
(12) Qi, D. F.; Fischbein, M.; Drndic, M.; Selmic, S. *Appl. Phys. Lett.* **2005**, 86(9).
(13) Zaban, A.; Micic, O. I.; Gregg, B. A.; Nozik, A. J. *Langmuir* **1998**, *14* (12), 3153−3156.
(14) Greenham, N. C.; Peng, X. G.; Alivisatos, A. P. *Phys. Rev. B* **1996**, *54* (24), 17628−17637.
(15) Zhang, S.; Cyr, P. W.; McDonald, S. A.; Konstantatos, G.; Sargent, E. H. *Appl. Phys. Lett.* **2005**, *87* (23).
(16) Maria, A.; Cyr, P. W.; Klern, E. J. D.; Levina, L.; Sargent, E. H. *Appl. Phys. Lett.* **2005**, *87* (21).
(17) Murphy, J. E.; Beard, M. C.; Nozik, A. J. *J. Phys. Chem. B* **2006**, *110* (50), 25455−25461.
(18) Talapin, D. V.; Murray, C. B. *Science* **2005**, *310* (5745), 86−89.
(19) Wehrenberg, B. L.; Yu, D.; Ma, J. S.; Guyot-Sionnest, P. *J. Phys. Chem. B* **2005**, *109* (43), 20192−20199.
(20) Wehrenberg, B. L.; Guyot-Sionnest, P. *J. Am. Chem. Soc.* **2003**, *125* (26), 7806−7807.
(21) Yu, D.; Wang, C. J.; Guyot-Sionnest, P. *Science* **2003**, *300* (5623), 1277−1280.
(22) Urban, J. J.; Talapin, D. V.; Shevchenko, E. V.; Murray, C. B. *J. Am. Chem. Soc.* **2006**, *128* (10), 3248−3255.
(23) Yu, W. W.; Falkner, J. C.; Shih, B. S.; Colvin, V. L. *Chem. Mater.* **2004**, *16* (17), 3318−3322.
(24) Dollefeld, H.; Weller, H.; Eychmuller, A. *J. Phys. Chem. B* **2002**, *106* (22), 5604−5608.
(25) Rabani, E.; Hetenyi, B.; Berne, B. J.; Brus, L. E. *J. Chem. Phys.* **1999**, *110* (11), 5355−5369.
(26) Yu, P. R.; Beard, M. C.; Ellingson, R. J.; Ferrere, S.; Curtis, C.; Drexler, J.; Luiszer, F.; Nozik, A. J. *J. Phys. Chem. B* **2005**, *109* (15), 7084−7087.
(27) Schedelbeck, G.; Wegscheider, W.; Bichler, M.; Abstreiter, G. *Science* **1997**, *278* (5344), 1792−1795.
(28) Leatherdale, C. A.; Bawendi, M. G. *Phys. Rev. B* **2001**, *63* (16).
(29) Jarosz, M. V.; Porter, V. J.; Fisher, B. R.; Kastner, M. A.; Bawendi, M. G. *Phys. Rev. B* **2004**, *70* (19).
(30) Stouwdam, J. W.; Shan, J.; vanVeggel, F. C. J. M.; Pattantyus-Abraham, A. G.; Young, J. F.; Raudsepp, M. *J. Phys. Chem. C* **2007**, *111* (3), 1086−1092.
(31) Franceschetti, A.; An, J. M.; Zunger, A. *Nano Lett.* **2006**, *6* (10), 2191−2195.
(32) Allan, G.; Delerue, C. *Phys. Rev. B* **2006**, *73* (20).
(33) Suzuki, N.; Sawai, K.; Adachi, S. *J. Appl. Phys.* **1995**, *77* (3), 1249−1255.

NL0708617